

Ultrafast Excited-State Isomerization Dynamics of 1,1'-Diethyl-2,2'-Cyanine Studied by Four-Wave Mixing Spectroscopy

Benjamin Dietzek,^{*,†} Niklas Christensson, Torbjörn Pascher, Tõnu Pullerits, and Arkady Yartsev

Department of Chemical Physics, Lund University, P. O. Box 124, SE-22100 Lund, Sweden

Received: December 12, 2006; In Final Form: March 14, 2007

Excited-state dynamics and solvent–solute interactions of 1,1'-diethyl-2,2'-cyanine iodine (1122C) in alcoholic solutions are investigated using time-integrated three-pulse photon-echo spectroscopy. 1122C serves as a model compound for ultrafast photoinduced isomerization—a key process in the light reception of plants, bacteria, and human vision. The photoreaction in 1122C is interrogated in dependence on solvent and excitation wavelength. The wavelength-dependent three-pulse photon-echo peak shift indicates strong alterations of the reaction pathways and points to the existence of a direct internal conversion channel in close proximity to the Franck–Condon point of absorption. The solvent-dependent S_1 – S_0 internal conversion time does not follow conventional sheared viscosity dependence, suggesting that the solvent local friction has to be considered to account for the observed isomerization kinetics. The concerted discussion of transient grating and three-pulse photon-echo peak-shift data allows us to derive a complete picture of the solvent–solute interaction-controlled photoreaction. The results obtained are related to other work on reactive systems and are discussed in the framework of multilevel response functions.

Introduction

Photoinduced structural changes of chromophore molecules play a key role in the light reception of plants, bacteria, and the human eye. The current interest in biological light receptors¹ and light-triggered enzymes² has renewed the efforts in studying photoinduced isomerization^{3–7}—a very basic, yet fundamental light-induced reaction. In studying model systems and comparing the results to biological systems, the function of the protein matrix in natural systems is to be unraveled,^{8–14} which is thought to be especially designed to steer the chemical reaction along the biologically functioning pathway.

Femtosecond time-resolved spectroscopy is a powerful tool to address detailed questions about processes mediated by enzymes and crucial for biological functioning, for example, reaction dynamics, signal transduction, and electron transfer.¹⁵ Especially three-pulse photon-echo spectroscopy offers great advantages to investigate intrachromophore and chromophore-environment dynamics, as the two characteristic signals conventionally obtained from such experiments, namely transient grating (TG) and three-pulse photon-echo peak shift (3PEPS), yield mainly complementary information.¹⁶ While the TG signal predominantly contains information about population dynamics, 3PEPS is sensitive to the amplitude and dynamics of environmental fluctuations.^{16–18} It was shown that for a simple electronic two-level system the 3PEPS directly follows the frequency correlation function.^{16,18} Time-integrated 3PEPS spectroscopy has been applied successfully to study solvation dynamics in a large range of solute–solvent combinations, glasses, proteins, and at interfaces.^{19–24} Furthermore, solvated electrons,²⁵ matrix-embedded polymers,^{26,27} and the flexibility

of an antibody-binding site²⁸ have been studied as have reactive electron-transfer systems in solution^{29,30} and in their biological protein environment.³¹

Cyanines, a class of polymethine dyes, have recently reattracted much attention as they constitute interesting model systems to investigate light-triggered excited-state isomerization (for an experimental overview, see 32). The range of photo-physical behavior extends from ultrafast excited-state isomerization in short-chain cyanines^{33–36} to slow bond twisting in the presence of a barrier³² including systems such as DDI,³⁷ whose S_1 potential resembles the key features of the bacteriorhodopsin excited-state potential.^{38,39} In agreement with the longstanding Bagchi–Fleming–Oxtoby (BFO) theory of bond-twisting motion,^{40,41} the excited-state lifetimes can be tuned drastically by the choice of solvent, i.e., the friction asserted on the solvated molecule by the environment.^{42–44} Furthermore, the formation of several photoisomers in cyanines, i.e., the presence of competing reaction channels, has been discussed.^{45,46} Theoretical studies yielded a detailed picture of the excited-state potential energy surfaces (ES-PES)^{47,48} and suggested routes to applying adaptive feedback control to influence the quantum yield of the isomerization reaction,⁴⁹ which very recently has been achieved experimentally.^{50–52}

In this study, 1,1'-diethyl-2,2'-cyanine iodine (1122C), a short-chain polymethine dye, is investigated by means of time-integrated three-pulse photon-echo spectroscopy. The absorption spectrum shows the characteristic features of cyanines: A main absorption located at 523 nm (19 120 cm^{-1}) is accompanied by two vibronic shoulders at 490 and \sim 460 nm corresponding to 20 420 and 21 740 cm^{-1} . However, the emission spectrum (Figure 1)—in contrast to characteristic emission spectra of longer chain cyanines^{32,36}—does not represent a mirror image of the absorption spectrum and is found to appear significantly more Stokes-shifted, broad (3390 cm^{-1}) and featureless. Emission of photoexcited 1122C molecules occurs over a wide range

* To whom correspondence should be addressed. Phone: (617) 253-7372. Fax: (617) 253-7030. E-mail: dietzek@mit.edu.

[†] Present address: Department of Chemistry, Massachusetts Institute of Technology, 77 Massachusetts Ave., Cambridge, MA 02139.

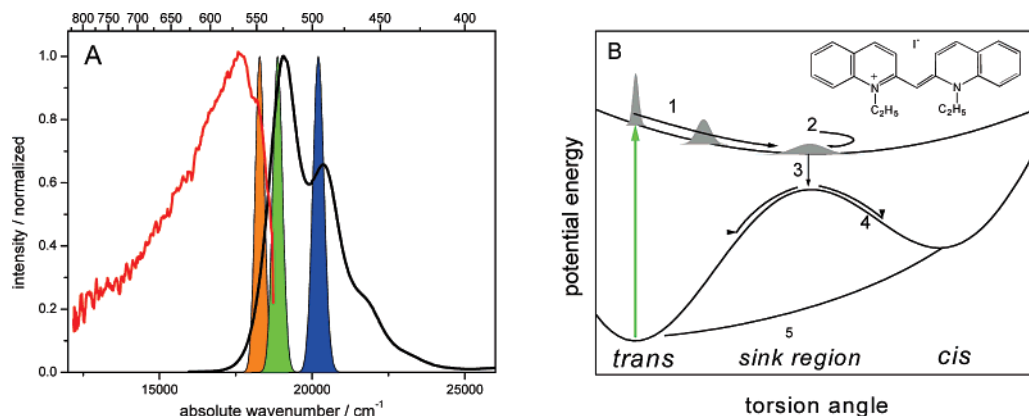


Figure 1. (A) Absorption and emission spectrum of 1122C in methanol. Dissolving 1122C in higher alcohols does not affect the shape of the absorption but slightly shifts the spectrum to lower wavenumbers. The pulses used in the experiment are schematically depicted. (B) Schematic representation of the excited-state bond-twisting motion.

of torsion angles. As the curvature of the excited-state potential was found to be much shallower than the curvature of the ground state, increasingly red-shifted emission wavelengths can be correlated with larger excited-state bond-twisting angles. Both visible absorption and emission are associated with a π - π^* transition, which is delocalized over the methine bridge. The observation of an unstructured and broad emission in concert with the large Stokes shift hints at severe changes during the relaxation from the absorption to the emission geometry and points to a fast excited-state isomerization process in 1122C. The general picture of this photoinduced bond-twisting motion as obtained from earlier pump-probe experiments³⁶ is outlined in Figure 1. After excitation of the trans form of 1122C at 523 nm and thus in the center of the 0-0 transition, the excited-state wavepacket broadens in about 100 fs and relaxes in a monodirectional bond-twisting motion to the sink region (process 1, Figure 1B). This directed excited-state bond-twisting motion takes place in about 1 ps when methanol is used as solvent. In the sink region and thus on a comparably flat part of the excited-state potential, random Brownian changes of the torsion angle take place in individual molecules, while the center of the angle distribution remains constant (process 2). The subsequent internal conversion (process 3) to the ground state is kinetically determined by the random bond-twisting motion at the bottom of the excited-state potential and can be characterized by a 4.9-ps time constant in methanol, while the ground-state recovery is found to be slightly slower, indicating cooling and bond-twisting motion on the ground-state potential (process 4). Furthermore, cis isomers are formed in the photoreaction, which relax back to the more stable trans form on a slower time scale (process 5).

Here, we investigate the excited-state dynamics in the reactive system 1122C and the coupling to its environment in dependence on solvent and excitation wavelength. A detailed picture of the light-induced reaction contains information on intrachromophore dynamics and solute-solvent interactions and will be related to the results of the pump-probe approach outlined above.³⁶ Furthermore, it will be shown that, besides TG and 3PEPS, the shape of the time-integrated echo reveals information about the dynamic processes.^{29,53} Finally, the wavelength-dependent long-term 3PEPS evolution points to the existence of two excited-state reaction pathways.

Experimental Section

The experimental setup has been described in detail previously.⁵³ Laser wavelengths at 548, 530, and 495 nm are used.

Thus 1122C is excited into the red shoulder, close to the maximum of the main absorption, and into the first vibronic shoulder, respectively. The laser pulses were characterized by intensity second-harmonic autocorrelation in a 30- μ m BBO crystal at the sample position to have typical autocorrelation widths of 40 fs (fwhm). Pulse energies of 50–100 nJ were employed corresponding to typically 5×10^{14} photons/(pulse \cdot cm²). 1122C was dissolved in solvents of spectroscopic grade as received from the supplier (Sigma-Aldrich). To avoid complications in the interpretation of the 3PEPS data due to propagation effects,⁵⁴ special care was taken to adjust the concentration such that each sample yielded an optical density of 0.2 at the particular excitation wavelength in a 0.2-mm quartz cuvette used for the measurements.⁵⁵

Response of a Three-Level System. The versatility of three-pulse photon-echo peak-shift spectroscopy is based on its property of directly mimicking transition energy fluctuations in a two-level system with a long-lived excited state.^{16,18} The electronic two-level system is linearly coupled to nuclear motions existing at low-frequency solvent modes and higher frequency vibrations of the chromophore.^{56,57} The nuclear system, usually referred to as a “bath”, can be represented as a quasicontinuous set of harmonic oscillators described via the multimode Brownian oscillator model.¹⁷ The transition energy fluctuations caused by the system-bath interactions determine the line-broadening function, which is used in the analytical expression for the response function $R(t)$.¹⁷ The TG and three-pulse photon-echo signals are associated with the absolute square of the third-order polarization emitted into the phase-matched directions $-k_1 + k_2 + k_3$ and $+k_1 - k_2 + k_3$. In the impulsive limit the polarization is equivalent to the third-order response function $R(\tau, T, t)$,¹⁷ where τ and T are the time delays between the first two pulses and between the second and third pulses, respectively; t is the time between the third pulse and the signal. $R(\tau, T, t)$ refers to the sum of different Feynman diagrams contributing to the signal. As has been outlined by Fleming and co-workers,²⁹ in a reactive system contributions of excited-state absorption (ESA) from more than one excited state, corresponding to different parts of the ES-PES in our work, have to be taken into account. Furthermore, response functions associated with a transiently populated state have to be weighted by an exponential factor, which reflects the population and depopulation kinetics of a particular state.^{11,29,30} As pathways resulting from ESA enter the total response function with a negative sign—opposite to ground-state absorption and stimulated emission pathways, which are associated with a positive sign¹⁷—

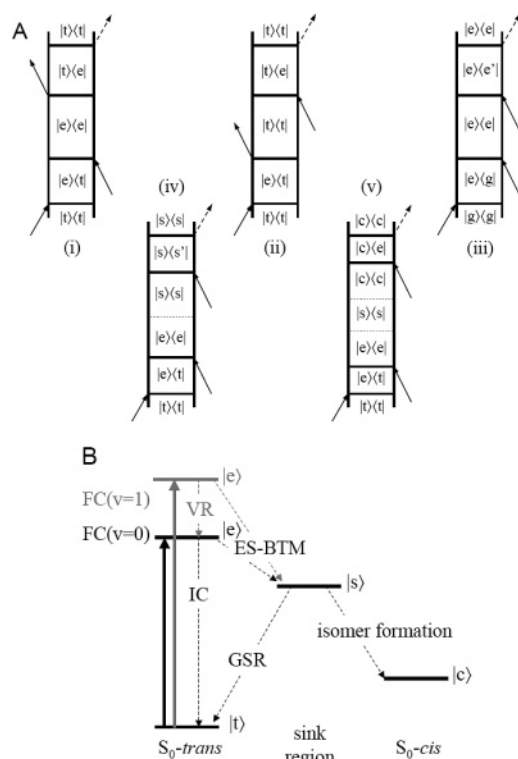


Figure 2. (A) Double-sided Feynman diagrams to account for the excited-state isomerization dynamics in 1122C. Diagram (i) results from stimulated emission from the Franck–Condon region, while (ii) describes ground-state contributions to the response. Diagram (iii) represents excited-state absorption from the Franck–Condon region, (iv) excited-state absorption from the sink region, and (v) cis-isomer absorption. (B) Schematic reduction of the potential energy diagram (Figure 1) to illustrate the origin of the diagrams shown in (A). Upon photoexcitation into the main absorption band, direct internal conversion back to the trans ground state (IC) is competing with excited-state bond-twisting motion (ES-BTM), which moves population to the sink region. From there (trans) ground-state recovery (GSR) is observed in concert with the isomer formation. Excitation into the vibronic shoulder leads to fast vibrational relaxation (VR) and a changed excited-state bond-twisting pathway.

interference between different contributions can lead to increasing TG and three-pulse photon-echo signals.^{11,29–31,58} The double-sided Feynman diagrams that contribute to the excited-state isomerization signal of 1122C are schematically presented in Figure 2. Diagrams (i) and (ii) are identical to those expected for a simple two-level system.¹⁷ However, it must be kept in mind that diagram (i) contributes only for about 500 fs to the signal, which is the time scale for motion out of the initially populated stimulated emission window close to the Franck–Condon point. In addition to (ii), diagram (iii) describing ESA from high-lying parts of the S_1 PES contributes to the signal only during the time that the excited-state population remains close to the Franck–Condon point (FC, Figure 2B). During population relaxation to the sink region, which takes place in about 1 ps in methanol, the weights of diagrams (i) and (iii) diminish and the contribution of ESA from the bottom of the ES-PES (diagram (iv)) grows in. It should be noted that no stimulated emission pathway contributes to the signal, when the excited-state population is located at the bottom of the ES-PES. In the sink region the S_0 and S_1 potentials are approaching and thus their energetic difference tends to zero. Furthermore, the broken conjugation along the methine bridge and a charge-transfer character of the state corresponding to the sink geometry of the molecules drastically reduce the dipole moment of

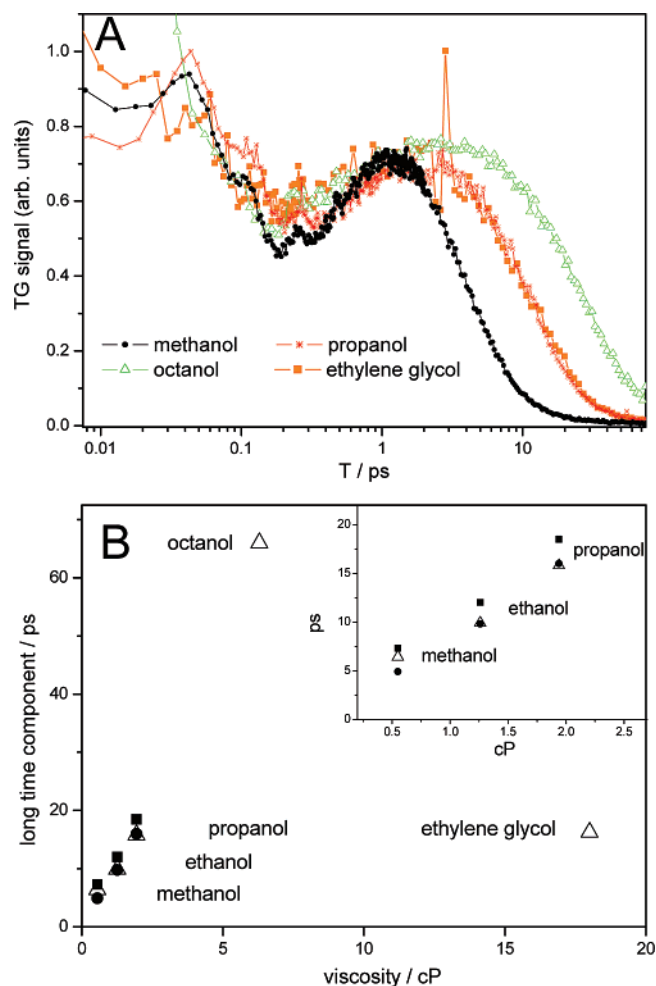


Figure 3. (A) TG signal of 1122C dissolved in methanol, propanol, octanol, and ethylene glycol measured at 548 nm.⁵⁵ (B) Time constants fitted to the long-term exponential decay of the 548-nm TG signals are plotted as a function of macroscopic solvent viscosity (triangles) and compared to the time constants for excited-state absorption decay (circles) and ground-state recovery (squares) as obtained from transient absorption measurements.^{36,52}

emission. As the cis isomer is found to absorb in the range of laser wavelengths used in this study,³⁶ diagram (v) gains weight to the overall response function upon S_1 – S_0 internal conversion. The kinetics of internal conversion is determined by the time it takes the system to encounter the conical intersection at the bottom of the ES-PES—a process that has been characterized by a 4.9-ps time constant in methanol. Subsequent to internal conversion, bond-twisting motion on the ground-state potential leads to cis-isomer formation. Concertedly, the trans ground state is partially refilled, which in turn diminishes the weight of the ground-state pathway (ii). At long population times in our experiment (some 10 ps), the signal results from diagrams (ii) and (v), associated with the cis ground-state population and trans ground-state hole.

Results and Discussion

Transient Grating Signals. Figure 3A displays the TG signal recorded at 548 nm, i.e., in the low-energy flank of ground-state absorption, of 1122C dissolved in various solvents. Some general features of the strongly nonexponential kinetics can be observed: An initial ultrafast (~ 100 fs) decay is observed for all solvents used. It should be noted that this decay is found to take place on a time scale more than 2 times longer than the

so-called coherent artifact, which arises from nonsequential pathway contributions and whose temporal profile is completely determined by the convolution of the three sub-30 fs pulses.^{60,61} The 100-fs decay, which corresponds to ultrafast population loss from the photoexcited Franck–Condon window, is followed by an intermediate component, which appears as a rise of the transient grating signal. The corresponding rise time is strongly solvent dependent and ranges from 280 fs in methanol to ~1.5 ps in octanol. Thus, its solvent viscosity dependence qualitatively matches the trend apparent in the long-time decay of the signal (Figure 3). Having reached an apparent plateau, the signal decays on a long time scale with a strongly solvent-dependent time constant, which reveals values between 6.4 and 66 ps in methanol and octanol, respectively. Independent of the solvent used, strong oscillatory components are superimposed to the multiexponential decay pattern. In order to evaluate the data quantitatively, the square root of the transient grating signal was fit to a sum of exponentials. TG measures the time-integrated absolute square of the third-order nonlinear response of the system, in contrast to transient absorption, where the signal due to the intrinsic heterodyned detection is proportional to the imaginary part of the response only. Therefore, in order to extract time constants directly related to the system dynamic, the square root of the TG data is subjected to fitting.¹⁶ The sum of exponentials used as a fitting function is not meant to prove or disregard any model, as excited-state bond-twisting motion is predicted to be strongly nonexponential.^{40,41} However, considerable insight into the underlying physics can be gained.

The time constants obtained for the long-term TG-signal decay coincide excellently with the time constants for excited-state-absorption (ESA) decay as obtained from pump–probe (PP) measurements⁴³ (Figure 3B). Therefore, it is concluded that the slow process visible in the data is associated with the internal conversion, whose dynamics is determined by the time scale of Brownian torsional motion at the bottom of the ES-PES. Based on a correlation of time scales from PP and TG measurements, we can also assign the other kinetic components visible in the TG signal to molecular processes: The initial sub-100 fs decay is associated with the broadening of the initially prepared excited-state wavepacket and a reduction of the stimulated emission (SE) contribution, i.e., diagram (i). The following TG-signal rise originates from downhill relaxation of the excited-state population from the FC point to the sink region, interestingly manifesting itself as a rise in the TG-signal amplitude. As the ground-state hole—diagram (ii)—contributes to the signal at any time until completion of the photoreaction, the ESA pathways—diagrams (iii) and (iv)—must be responsible for the observed differences in TG amplitude. Therefore, the rising signal amplitudes indicate that the ESA cross section close to the FC point is larger than in proximity to the sink region. In earlier measurements, any information about ESA cross sections was hidden under the strong ground-state bleach signal in the PP data, which dominated the appearance of the differential absorption spectra in this spectral region.³⁶

In the sink region the system encounters the conical intersection and relaxes down to the ground state. As mentioned above, the dynamics of internal conversion is determined by random changes of the torsion angle at the bottom of the ES-PES. The long-term TG data representing the kinetics of internal conversion features decay constants between 6.4 and 66 ps in agreement with characteristic times of ESA decay and trans ground-state recovery (Figure 3B). Finally, thermally driven cis–trans back-isomerization and equilibration of the ground-state population occurs within 500 ps, a time scale remarkably

short compared to that for long-chain cyanines. Time-resolved differential absorption experiments determined the isomerization yield of 1122C in methanol to be 27% by fitting the differential absorption spectrum at long delay times as a sum of two absorption spectra of the same overall shape.³⁶ However, the single color data presented here do not show a significant long-lived TG signal.

For population times longer than the excited-state lifetime (i.e., $T > 5$ ps), the impulsive 3PE signal is governed by the response functions (ii) and (v) (Figure 2A). These response functions differ in the number of interactions from the right-hand site and will thus contribute with opposite phase (or sign) and consequently interfere destructively. It is often assumed that the cis and trans isomers have the same spectral shape, which means that they are subject to the same bath fluctuations and hence have a common line shape function. Ignoring slow dynamics like cooling of the trans (and cis) ground state, we find, given the assumptions above, that the response functions have identical temporal evolution and differ in magnitude by a population prefactor reflecting the branching ratio. We also need to account for the frequency shift of the cis isomer by introducing wavelength-dependent amplitudes of the response functions. If the shift were negligible compared to the width of the absorption spectrum, the TG signal would vanish for a 50/50 split, even though there is no complete recovery of the trans ground state. For finite shifts we expect wavelength-dependent interference between the complex-valued response functions and no general statement about the relation between cis and trans isomers can be made.⁶¹ The low value of the TG signal at long times should thus not be interpreted as absence of trans ground-state hole. Since the shift between the isomers in the present study is small (530 cm^{-1}) compared to the width of the absorption and the pulse spectrum, we cannot resolve the wavelength dependence of this interference effect. Given this wavelength-dependent interference, we conclude that TG is inferior to a differential absorption pump–probe experiment in determining the isomerization yield.

In order to validate the dependence of the appearance of the ultrafast isomerization on the viscosity over a larger range of viscosities, 1122C dissolved in ethylene glycol was included in the 548-nm-excitation experiments (Figure 3). Surprisingly, the overall kinetic picture as seen in the TG kinetics is very similar to the one obtained for 1122C in propanol, though the bulk viscosity of ethylene glycol is about an order of magnitude higher than the viscosity of propanol. Following the prediction of BFO theory, 1122C Brownian torsional motion is expected to be an order of magnitude slower in ethylene glycol compared to propanol. Nonetheless, in both solvents the long-term signal decay representing the kinetics of internal conversion, i.e., Brownian torsion motion, can be characterized by a ~15-ps time constant. This proves that the bond-twisting motion is *not* determined by macroscopic viscosity but instead solvent local friction has to be considered in describing the effect of the solvent on the reaction correctly.^{62–65}

While the TG signal of 1122C in linear, short-chain alcohols recorded at 530 nm exhibits features qualitatively and quantitatively identical with those at 548 nm (Figure 4A), the data measured at 495 nm show a behavior qualitatively different from that of the signals obtained for longer excitation wavelengths (Figure 4B). No distinct rise is visible anymore; instead the picosecond component is observed with a positive sign. In line with the discussion outlined above, the absence of the rise component for 1122C in the linear alcohols can be accounted for by invoking a strong ESA for geometries corresponding to

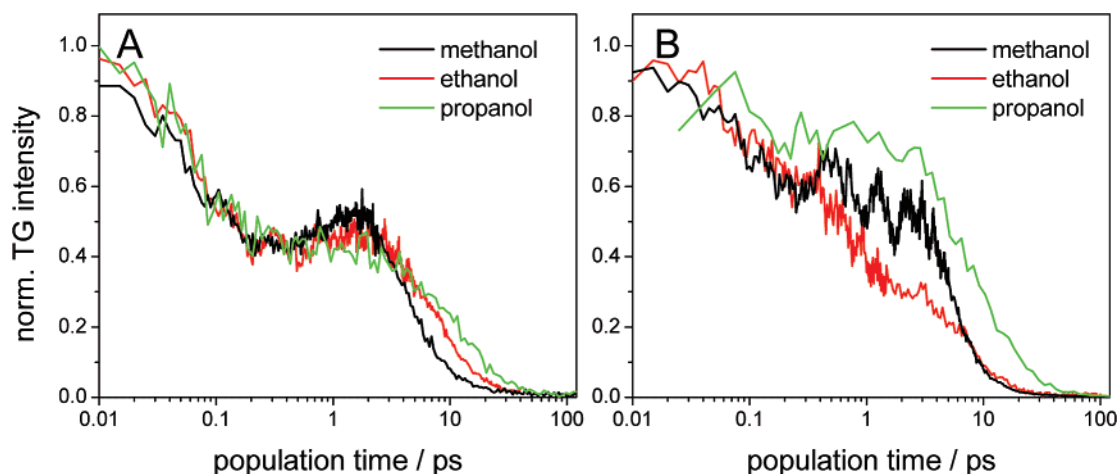


Figure 4. TG signal of 1122C in various solvents recorded at (A) 530- and (b) 495-nm excitation.

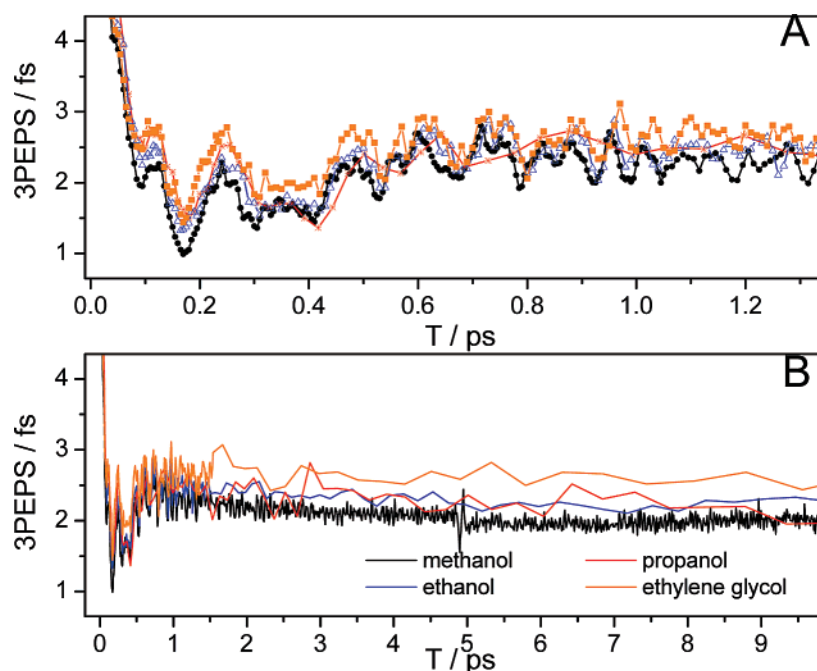


Figure 5. 3PEPS signal for short population times recorded at 548 nm for 1122C in various solvents.

larger torsion angles compared to the situation at the FC point. This comparison indicates that the equilibrated population characterized by large torsion angles is not completely spectrally dark. When approaching the 90°-twist geometry, the stimulated emission cross section is found to drop drastically³⁶ due to the increasingly broken conjugation of the methine bridge and a growing charge-transfer character of the state.⁶⁶ However, the findings presented here indicate that the excited-state population in proximity of the sink region of cyanines might be indirectly spectroscopically accessible when it is possible to separate ESA dynamics from—most likely—dominating ground-state bleach contributions, which appear in the same spectral range. Though the quantification of ESA cross sections is hampered in spectral regions in which ground-state bleach contributes to the signals, assuming different ESA contributions at 495 nm compared to 530 and 548 nm, the wavelength-dependent TG signal can be explained by the change in probe wavelengths.

3PEPS Measurements. Figure 5 displays the 3PEPS data recorded at 548 nm in different solvents. Independent of solvent, an overall identical trend is observed: An ultrafast decay component (~ 100 fs) is followed by a rise, which can be characterized by a subpicosecond time constant. Superimposed

to the multiexponential behavior, high-frequency oscillations can be seen, which—as discussed below—are identical to those observed in the TG data (Figures 3A and 4A). Subsequent to the rise component, a slow decay results in a quasistatic level of the peak shift, which extends over the entire range of population times accessible within the experimental signal-to-noise ratio. The static long-term level has a larger amplitude for 1122C in ethylene glycol compared to the *n*-alcohols.

Comparing the peak shift at different excitation wavelengths (Figure 6), it can be seen that excitation close to the maximum of absorption (530 nm) yields results very similar to those of red excitation (548 nm) independent of the solvent used. However, quantitative differences can be seen in Figure 6: The amplitude of the plateau level is slightly higher and the amplitude of high-frequency oscillations is reduced for red excitation compared to the excitation close to the absorption peak. At 495 nm a qualitatively different peak-shift behavior is observed: The initial decay of peak shift is faster and contributes to the overall signal with a larger amplitude, leading to essentially zero peak shift in about 500 fs. Furthermore, no high-frequency intramolecular oscillations are apparent, and finally and most remarkably a strong peak-shift recovery can be seen

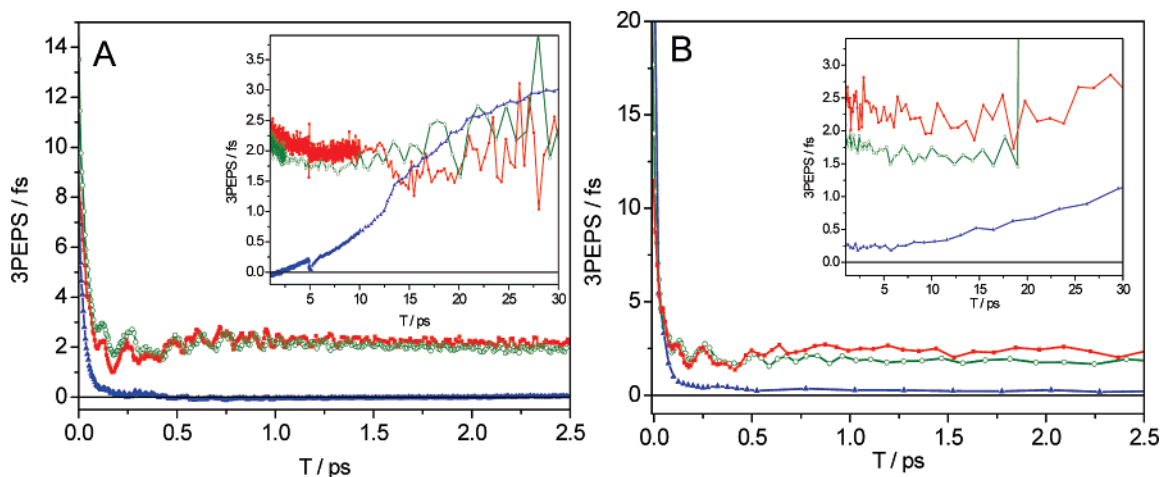


Figure 6. Comparison of 3PEPS signals measured at different excitation wavelengths, 548 (red), 530 (green), and 495 nm (blue), in (A) methanol and (B) propanol. The inset highlights the long-population-time dependence. (The spike in the 3PEPS signal recorded at 530 nm seen in the inset of panel B is due to noise imposed by fitting photon-echo signals of drastically reduced amplitudes.)

at long delay times. The onset of the later recurrence and its characteristic time constant is solvent dependent (Figure 6) and follows the overall trend of viscosity-dependent internal conversion as obtained from the TG measurements.⁶⁷

Before discussing the rising peak shift recorded at 495 nm at long population times, we will focus on the discussion of the 3PEPS signal at longer excitation wavelengths. Expectedly, the peak shift does not reflect the solvent frequency correlation function, as 1122C does not constitute a simple two-level system.^{16–18} In fact, the peak shift reflects the dynamic processes of the reactive system^{11,29–31} and the more complex level system (Figures 1 and 2) has to be invoked to account for the observed dynamics. Upon photoexcitation, a rather narrow excited-state wavepacket experiences the derivative of the ES-PES along the reaction coordinate and interactions with the solvent. Librational solvation dynamics, i.e., reversible small angle free rotations of the solvent molecules in the first solvation shell,⁶⁸ cause the wavepacket to broaden. As the solvation dynamics is associated with a loss of frequency memory in solvated 1122C, the process is apparent as a decay of 3PEPS amplitude. This initial ~ 100 fs decay component is insensitive to the solvent viscosity, further corroborating the assignment of this process to librational solvation, a process found to be the same in alcohols over a large range of chain lengths.⁶⁹

Following the initial ultrafast process, a sub-1 ps rise of the peak shift is observed. According to Jimenez and co-workers,¹¹ this intermediate rise can be understood in terms of reduction of the ground-state contribution to the response function due to internal conversion together with the effect of excited-state wavepacket motion. PP experiments showed that the motion of the initially populated transient SE window takes place on a 500-fs time scale for 1122C dissolved in various *n*-alcohols.⁴³ Hence, in analogy to the observed picosecond increase of the TG signal, the time-dependent contributions of different response functions associated with the reactive scheme (Figures 1 and 2) leads to an increase of the peak shift. Therefore, the observation of the peak-shift recurrence indicates the reactive nature of the multilevel system and illustrates that the peak shift in 1122C does not follow the frequency correlation function as predicted for a simple two-level system.^{16–18}

When excited-state isomerization is complete, i.e., after relaxation to the sink region, a static peak-shift level is reached. The solvent dependence of the long-time peak shift reflects different levels of inhomogeneity in different solvents. The transient grating data presented here and the results of a related

PP study⁴³ show that changes in torsion angle are strongly coupled to changes in the solvent structure surrounding the solute molecules. As the interconversion of different parts of the population characterized by their torsion angles is hindered in more viscous solvents, a higher level of inhomogeneity is observed after the initial excited-state photoreaction. When comparing the static peak-shift level for a given solvent for excitation at 548 and 530 nm (Figure 5), it is apparent that the peak shift is slightly higher for the red-most excitation. This finding is in line with the results reported by Fleming and co-workers^{56,57} and is related to the different subpopulations being addressed with a change in excitation wavelength. In 1122C the absorption characteristic of an individual molecule is determined by its torsion angle. Thus, molecules being excited at 548 nm are contained in a different subpopulation than those absorbing at 530 and 495 nm. Hence, scanning the excitation wavelength different distributions of molecules are addressed, which show different rephrasing capabilities and consequently different peak-shift values.

As mentioned previously, recording the peak shift at 495 nm yields a drastically altered overall picture: The initial decay of peak shift is faster compared to longer excitation wavelengths and no oscillations are superimposed to the kinetics. At intermediate population times ranging from about 500 fs to some picoseconds (depending on the solvent), nearly zero peak shift is observed. A comparison of the peak-shift level at intermediate time scales for different excitation wavelengths reveals that the trend of decreasing peak-shift values with decreasing excitation wavelength holds—as already detailed in comparing the peak-shift values at 548 and 530 nm.^{56,57} However, in order to account for the—compared to 530-nm excitation—drastically diminished 3PEPS amplitude, an argument given by Jimenez and co-workers is invoked.⁷⁰ In a recent photon-echo study performed on porphyrins with Soret band excitation, these authors report that the peak shift of two ideally degenerate transitions does not differ from the peak shift of a single transition. Nonetheless, if the degeneracy is lifted as in real porphyrins, the peak shift is reduced significantly.⁷⁰ In our experiments excitation at 495 nm leads to simultaneous interactions with the $0 \rightarrow 0$ and $0 \rightarrow 1$ vibrational levels in the S_1 state of 1122C. Along the lines suggested by Jimenez and co-workers,⁷⁰ in this experimental situation the data resembles the peak shift, where the splitting of the bands (1300 cm^{-1}) corresponds to the vibrational progression. We suggest that the excitation-wavelength dependence of the (almost static) peak-shift level at intermediate

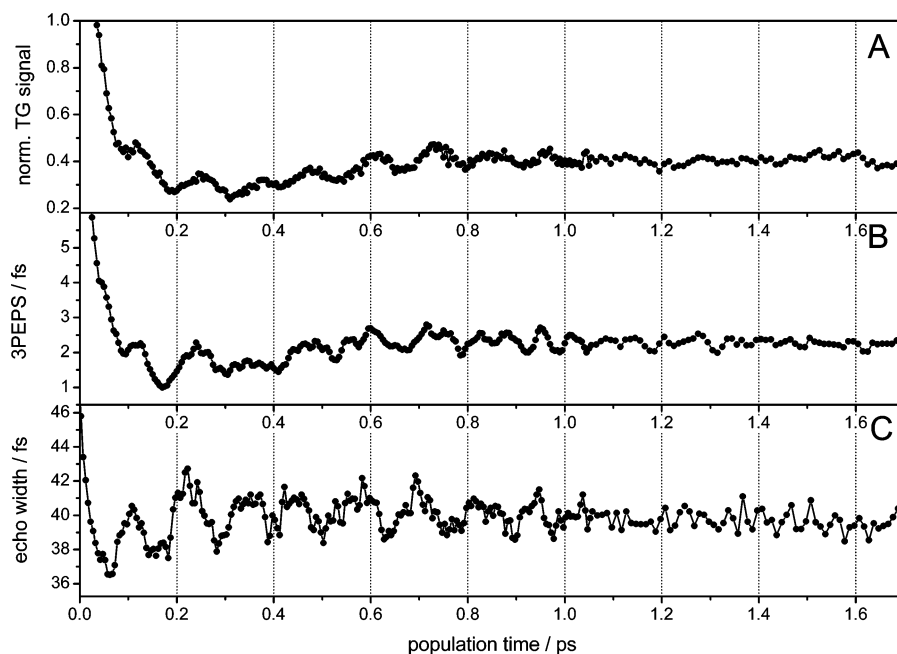


Figure 7. 1122C dissolved in methanol. Data constructed from the experiment performed at 548 nm. (A) TG, (B) 3PEPS, and (C) width of the three-pulse photon echo as a function of population time.

population times is related to three distinct effects, which have been discussed in literature: First, addressing different sub-populations within the overall ensemble has been found to diminish the overall peak-shift level.^{56,57} Second, excitation at 495 nm leads to the situation that two distinct nondegenerate transitions are experimentally addressed, which reduces the observed 3PEPS amplitude.⁷⁰ Finally, excitation of the vibrational shoulder at 495 nm leads to more vibrations being initially excited and vibrational dephasing leads to the extremely fast and dominant 3PEPS decay apparent in our data.¹⁶ The observed zero peak-shift level is consistent with reports on the excitation-wavelength dependence of the 3PEPS signal given in the literature and reflects the dominant coherence loss due to vibrational dephasing.¹⁶ Excitation at 495 nm adds extremely fast vibrational relaxation to the deactivation pathway, as indicated in Figure 2B. The rate of this process is fast compared to the internal conversion rate discussed above. Therefore, the characteristic picosecond recurrence is not observed when recording the 3PEPS signal at 495 nm.

Finally, a strong peak-shift recovery is observed at long delay times (Figure 6). This rise can be rationalized along the lines presented by Yang et al.³⁰ These authors presented calculations which show that the responses of molecules rapidly returning to the ground state and subsequently evolving via the ground-state pathway (ii) (Figure 2A) and molecules returning to the ground state after completion of the photoreaction can interfere. This interference is related to the different phase of the response function that has been acquired during the nuclear motion along the reaction path, involving pathways with a rapid return to the ground state via a direct internal conversion deactivation channel and pathways that engage the entire isomerization pathway. As the system remembers the history of the reaction and the phase difference acquired along the different pathways, the authors of ref 30 refer to this effect as the *nuclear history effect*. They showed that this effect gives rise to a prominent increase of the peak shift on long time scales.³⁰ Along these lines we interpret our results in terms of the nuclear history effect: Excitation at 495 nm and thus into the vibrational shoulder leads to significantly different starting conditions for the excited-state relaxation. An altered excited-state relaxation and thus a changed

reaction pathway is observed, which is most likely associated with larger scale nuclear motions on the ES-PES. Hence, under this experimental condition a strong long-time peak-shift recurrence is observed, which is not seen in the data recorded at 530 and 548 nm.

Following the argumentation given in ref 30, the appearance of the subpicosecond peak shift rise is coupled to the relation between the excited-state reaction rate and a rate of direct internal conversion to the ground state. Such a direct internal conversion pathway is an implicit result of recent theoretical calculations of the ES-PES of a model cyanine,^{47,49} and optimal control experiments by some of us have been explained along these lines.⁵¹ The ultrafast direct IC channel will together with ES-BTM contribute to the ultrafast 100-fs decay of the TG signal and will most likely dominate the process in the higher viscous solvents, in which torsion motion is drastically slowed. However, previous PP experiments were not capable of resolving this pathway,³⁶ most likely due to the limited temporal resolution used in this study. Nonetheless, the nuclear history effect might constitute a fundamental advantage of 3PEPS compared to PP experiments, in situations in which an ultrafast decay channel competes with a slower relaxation. As shown in ref 30, the interference between different reaction pathways is manifested on time scales longer than the actual characteristic time of the fast process. Hence, the visibility of the process is significantly enhanced. To the best of our knowledge, the data presented here constitute the first direct proof of a fast internal conversion channel in the photoreaction path of cyanines.

Intramolecular Vibrations in Transient Grating and 3PEPS Signals. Having discussed the overall appearance and manifestation of various kinetic processes in the TG and 3PEPS signals, we will now focus on the pronounced oscillation contributions that can be found in the experimental data (Figure 7). It is well established that intramolecular high-frequency modes are excited in a coherent four-wave mixing experiment, if the bandwidth of the laser pulses spans the 0–1 transition of the corresponding mode.^{56,57} These intramolecular vibrations have a molecular origin very distinct from that of the low-frequency phonons of the bath and appear as oscillatory contributions to the 3PEPS and TG signals.^{56,57} While excitation

at 530 nm leads to less pronounced oscillations compared to 548-nm excitation, the 495-nm kinetics show no high-frequency oscillations. However, some ~ 800 -fs modulation in the 495-nm TG signal is observed in methanol (Figure 4B), whose origin is unclear at the present stage of the study but is subject to further investigations. The oscillations observed in the 548-nm TG data extend for about 1 ps; i.e., their damping is roughly correlated with the time of arrival in the sink region. The insensitivity of the oscillation pattern (Figure 5) to the solvent friction indicates that the oscillations are not related to torsion, which has been shown to be strongly solvent dependent.^{40,41,43} Furthermore, it is remarkable that oscillations appear for such a long time and extend during the entire torsional downhill motion. Ground-state hole broadening and excited-state wavepacket spreading in methanol take place on a time scale of 200 and 100 fs, respectively.³⁶ As has been discussed, both processes are driven by the solvent–solute interactions. Thus, the time scale of solvent–solute interaction distributing the initially photoprepared selection of torsion angles over a wider range of geometric structures is much faster than the time scale of oscillational damping (Figure 7). This indicates that the interaction of the solvent with torsional motion is distinctly different from the coupling of other normal modes to the environment.

Finally, Figure 7C features the width of the time-integrated photon echo as a function of population time, where the high-frequency intramolecular vibrations are also reflected.⁵³ Furthermore, the echo width exhibits a recurrence on the subpicosecond time scale very similar to the recurrence induced by the reactive pathways and seen in the 3PEPS signal and the TG signal. Thus, besides containing information on the intramolecular vibrations of the solute,⁵³ the echo width reveals information on the reactive nature of the system as well.²⁹ The detailed appearance of the population-time dependence of the width, i.e., the slightly shifted beating pattern compared to the 3PEPS oscillations and the apparently shortened recurrence time, is the subject of current investigations and will be published in forthcoming work.

Joint View on Ultrafast Excited-State Isomerization of 1122C. Based on a correlation of time scales from PP and photon-echo measurements, we can assign the decay components to their kinetic counterparts as determined from PP spectroscopy: Upon photoexcitation at the central and red parts of the absorption band librational motion of the solvent immediately surrounding 1122C molecules results in the ultrafast broadening of the excited-state wavepacket within 100 fs.³⁶ This process, which is independent of solvent viscosity,⁶⁹ is associated with a loss of coherence and therefore is seen as a rapid decay of the peak-shift signal. The motion of the excited-state wavepacket from the FC point to the bottom of the ES-PES in methanol was found by PP measurements to be complete in about 1 ps.³⁶ During this process the contribution from the ground state to the photon-echo signal remains unchanged; however, the contribution from ESA changes. The differences in ESA from the FC point and the sink region are manifested in the increase of the TG signal. The rise of the 3PEPS signal is related to the ultrafast wavepacket motion out of the FC window, which changes the time-dependent contributions of different Feynman diagrams.^{11,29–31} Internal conversion from the sink region to the ground-state potential is seen as a decay of the TG signal with time constants being strongly solvent dependent, ranging from 6 to 66 ps in methanol and octanol, respectively. The observed decay characteristics match the decay times of ESA and ground-state recovery as determined by PP spectroscopy.^{36–43} Despite their very different macroscopic

viscosities, propanol and ethylene glycol apparently affect the excited-state isomerization in 1122C in a quantitatively similar way. This surprising finding underpins the importance in considering local friction instead of macroscopic viscosity when discussing the solvent–solute interactions during photoinduced isomerization. Finally, pronounced high-frequency oscillations in the TG signal, 3PEPS, and the echo width are observed for the time scale of motion to the bottom of the ES-PES. The remarkably slow damping of the intramolecular vibrations compared to the strong damping of the bond-twisting motion indicates that the coupling of the torsion motion to the solvent is intrinsically different from other 1122C vibrations.

When excitation into the first vibronic shoulder is used, a quantitatively different overall picture is obtained: ultrafast vibrational relaxation and dephasing of different excited vibrations lead to a shortening of the initial decay of the 3PEPS and to the close-to-zero value of the peak shift at intermediate population times. Furthermore, efficient vibrational dephasing destroys the appearance of high-frequency vibrations in the photon-echo data.^{56,57} Neither in TG nor in 3PEPS is a subpicosecond recurrence observed. The lack of a TG rise is explained by different contributions of ESA when changing the excitation wavelength. In contrast, the extremely rapid vibrational relaxation is responsible for the nonapparent peak-shift recurrence. When initially excited molecules return to the ground state after the photoreaction, the nuclear history effect gives rise to the pronounced long-time increase of the peak shift.³⁰ This process demands the presence of two distinct deactivation channels, i.e., the photoreaction pathway and a direct and fast deactivation of S_1 molecules. The latter is most likely represented by a direct internal conversion occurring in close proximity to the FC point. A direct internal conversion pathway in cyanines is an implicit result of recent theoretical calculations^{47,49} and has recently been invoked to interpret an optimal control experiment.⁵¹ Nonetheless, this study presents to the best of our knowledge the first direct spectroscopic evidence for the existence of such a fast internal conversion channel.

In conclusion, the study presented here monitors photoinduced barrierless isomerization in 1122C as a function of solvent and excitation energy. The results are in excellent agreement with a previous transient absorption study but reveal much more detailed insight into the isomerization mechanism and the properties of the photoexcited solvated dye. Therefore, we believe that they constitute an important contribution in the advanced understanding of the photophysics of cyanines—a paradigm class of molecules when discussing the biologically highly relevant process of excited-state isomerization.

Acknowledgment. We thank Prof. Villy Sundström and Dr. Petter Persson for many helpful and stimulating discussions. This work was financially supported by the Swedish Research Council and the Alice and Knut Wallenberg Foundation.

References and Notes

- (1) Sundström, V. *Prog. Quantum Electron.* **2000**, *24*, 187 and references therein.
- (2) Heyes, D. J.; Hunter, C. N. *Trends Biochem. Sci.* **2005**, *30*, 642.
- (3) Glassbeck, M.; Zhang, H. *Chem. Rev.* **2004**, *104*, 1929.
- (4) Espagne, A.; Paik, D. H.; Changelnet-Barret, P.; Martin, M. M.; Zewail, A. H. *ChemPhysChem* **2006**, *7*, 1717.
- (5) Schultz, T.; Quenneville, J.; Levine, B.; Toniolo, A.; Martinez, T. J.; Lochbrunner, S.; Schmitt, M.; Shaffer, J. P.; Zgierski, M. Z.; Stolow, A. *J. Am. Chem. Soc.* **2003**, *125*, 8098.
- (6) Usman, A.; Mohammed, O. F.; Nibbering, E. T. J.; Dong, J.; Solntsev, K. M.; Tolbert, L. M. *J. Am. Chem. Soc.* **2005**, *127*, 11214.
- (7) Cervetto, V.; Bregy, H.; Hamm, P.; Helbing, J. *J. Phys. Chem. A* **2006**, *110*, 11473.

- (8) Schoenlein, R. W.; Pateanu, L. A.; Mathies, R. A.; Shank, C. V. *Science* **1991**, 262, 4012.
- (9) Kukura, P.; McCamant, D. W.; Yoon, S.; Wandschneider, D. B.; Mathies, R. A. *Science* **2005**, 310, 1006.
- (10) Prokhorenko, V. I.; Nagy, A. M.; Waschuk, S. A.; Brown, L. S.; Birge, R. R.; Miller, R. J. D. *Science* **2006**, 313, 1257.
- (11) Jimenez, R.; Romesberg, F. E. *J. Phys. Chem. B* **2002**, 106, 9172.
- (12) Lang, M. J.; Jordanides, X. J.; Song, X.; Fleming, G. R. *J. Chem. Phys.* **1999**, 110, 5884.
- (13) Gai, F.; Hasson, K. C.; McDonald, J. C.; Anfinrud, P. A. *Science* **1998**, 279, 1886.
- (14) Larsen, D. S.; van Grondelle, R. *ChemPhysChem* **2005**, 6, 828.
- (15) Sundstrom, V.; Pullerits, T.; van Grondelle, R. *J. Phys. Chem. B* **1999**, 103, 2327.
- (16) Joo, T.; Jia, Y.; Yu, J. Y.; Land, M. J.; Fleming, G. R. *J. Chem. Phys.* **1996**, 104, 6089.
- (17) Mukamel, S. *Principles of Nonlinear Optical Spectroscopy*; Oxford University Press: Oxford, 1995.
- (18) deBoeij, W. P.; Pshenichnikov, M. S.; Wiersma, D. A. *Chem. Phys. Lett.* **1996**, 253, 53.
- (19) de Boeij, W.; Pshenichnikov, M. S.; Wiersma, D. A. *Annu. Rev. Phys. Chem.* **1998**, 49, 99.
- (20) Fleming, G. R.; Cho, M. *Annu. Rev. Phys. Chem.* **1996**, 47, 109.
- (21) Agrawal, R.; Rizvi, A. H.; Prall, B. S.; Olsen, J. D.; Hunter, C. N.; Fleming, G. R. *J. Phys. Chem. A* **2002**, 106, 7573.
- (22) Jordanides, X. J.; Lang, M. J.; Song, X.; Fleming, G. R. *J. Phys. Chem. B* **1999**, 103, 7995.
- (23) deBoeij, W. P.; Pshenichnikov, M. S.; Wiersma, D. A. *J. Phys. Chem.* **1996**, 100, 11806.
- (24) Bursing, H.; Ou, D.; Kundu, S.; Vohringer, P. *Phys. Chem. Chem. Phys.* **2001**, 3, 2378.
- (25) Baltuska, A.; Emde, M. F.; Pshenichnikov, M. S.; Wiersma, D. A. *J. Phys. Chem. A* **1999**, 103, 10065.
- (26) Yang, X.; Dykstra, T. E.; Scholes, G. D. *Phys. Rev. B* **2005**, 71, 045203.
- (27) Dykstra, T. E.; Kovalevskij, V.; Yang, X.; Scholes, G. D. *Chem. Phys.* **2005**, 318, 21.
- (28) Jimenez, R.; van Mourik, F.; Yu, J. Y.; Fleming, G. R. *J. Phys. Chem. B* **1997**, 101, 7350–7359.
- (29) Yang, M.; Ohta, K.; Fleming, G. R. *J. Chem. Phys.* **1999**, 110, 10243.
- (30) Xu, Q.-H.; Scholes, G. D.; Yang, M.; Fleming, G. R. *J. Phys. Chem. A* **1999**, 103, 10348.
- (31) Groot, M. L.; Yu, J. Y.; Agarwal, R.; Norris, J. R.; Fleming, G. R. *J. Phys. Chem. B* **1998**, 102, 5923.
- (32) Meyer, Y. H.; Pittman, M.; Plaza, P. *J. Photochem. Photobiol., A* **1998**, 114, 1.
- (33) Aberg, U.; Akesson, E.; Sundstrom, V. *Chem. Phys. Lett.* **1993**, 215, 388.
- (34) Yartsev, A.; Alvarez, J. L.; Aberg, U.; Sundström, V. *Chem. Phys. Lett.* **1995**, 243, 281.
- (35) Dietzek, B.; Pascher, T.; Yartsev, A. Accepted for publication in *J. Phys. Chem. B*.
- (36) Dietzek, B.; Yartsev, A.; Tarnovsky, A. N. *J. Phys. Chem. B* **2007**, 111, 4520.
- (37) Tarnowski, A. N. Private communication.
- (38) Gai, F.; McDonald, C.; Anfinrud, P. A. *J. Am. Chem. Soc.* **1997**, 119, 6201.
- (39) Ruhmann, S.; Hou, B.; Friedman, N.; Ottolenghi, M.; Sheves, M. *J. Am. Chem. Soc.* **2002**, 124, 8854.
- (40) Bagchi, B.; Fleming, G. R.; Oxtoby, D. W. *J. Chem. Phys.* **1983**, 78, 7375.
- (41) Bagchi, B.; Fleming, G. R. *J. Phys. Chem.* **1990**, 94, 9.
- (42) Xu, Q. H.; Fleming, G. R. *J. Phys. Chem. A* **2001**, 105, 10187.
- (43) Dietzek, B.; Yartsev, A.; Tarnovsky, A. N. Manuscript in preparation.
- (44) Alvarez, J. L.; Yartsev, A.; Aberg, U.; Akesson, E.; Sundström, V. *J. Phys. Chem. B* **1998**, 102, 7651.
- (45) Nuernberger, P.; Vogt, G.; Gerber, G.; Improta, R.; Santoro, F. *J. Chem. Phys.* **2006**, 125, 044512.
- (46) Vogt, G.; Nuernberger, P.; Gerber, G.; Improta, R.; Santoro, F. *J. Chem. Phys.* **2006**, 125, 044513.
- (47) Sanchez-Galvez, A.; Hunt, P.; Robb, M. A.; Olivucci, M.; Vreven, T.; Schlegel, H. B. *J. Am. Chem. Soc.* **2000**, 122, 2911.
- (48) Improta, R.; Santoro, F. *J. Chem. Theory Comput.* **2005**, 1, 215.
- (49) Hunt, P. A.; Robb, M. A. *J. Am. Chem. Soc.* **2005**, 127, 5720.
- (50) Vogt, G.; Krampert, G.; Niklaus, P.; Nuernberger, P.; Gerber, G. *Phys. Rev. Lett.* **2005**, 94, 068305.
- (51) Dietzek, B.; Bruggemann, B.; Pascher, T.; Yartsev, A. *Phys. Rev. Lett.* **2006**, 97, 258301.
- (52) Dietzek, B.; Bruggemann, B.; Pascher, T.; Yartsev, A., manuscript in preparation.
- (53) Dietzek, B.; Christensson, N.; Kjellberg, P.; Pascher, T.; Pullerits, T.; Yartsev, A. *Phys. Chem. Chem. Phys.* **2007**, 9, 701.
- (54) Christensson, N.; Dietzek, B.; Pascher, T.; Yartsev, A.; Pullerits, T., manuscript in preparation.
- (55) For technical reasons, the TG signal of 1122C in octanol was measured in a 1-mm-thick cuvette. However, TG signals, in contrast to 3PEPS data, are not noticeably affected by propagation effects. Due to the pronounced propagation distortion of the 3PEPS signal in long-pathway samples,⁵⁴ the discussion of the data is excluded from the paper and only experiments yielding 3PEPS data using a 0.2-mm sample cell are discussed.
- (56) Ohta, K.; Larsen, D. S.; Yang, M.; Fleming, G. R. *J. Chem. Phys.* **2001**, 114, 8020.
- (57) Larsen, D. S.; Ohta, K.; Xu, Q. H.; Cyrier, M.; Fleming, G. R. *J. Chem. Phys.* **2001**, 114, 8008.
- (58) Nagasawa, Y.; Watanabe, A.; Takikawa, H.; Okada, T. *J. Phys. Chem. A* **2003**, 107, 632.
- (59) Rentsch, S. K. *Chem. Phys.* **1982**, 69, 81.
- (60) Ferwerda, H. A.; Terpstra, J.; Wiersma, D. A. *J. Chem. Phys.* **1989**, 91, 3296.
- (61) Xu, Q. H.; Ma, Y. Z.; Fleming, G. R. *J. Phys. Chem. A* **2002**, 106, 10755.
- (62) Akesson, E.; Hakkarainen, A.; Laitinen, E.; Helenius, V.; Gillbro, T.; Korppi-Tommola, J.; Sundstrom, V. *J. Chem. Phys.* **1991**, 95, 6508.
- (63) Korppi-Tommola, J. E. I.; Hakkarainen, A.; Hukka, T.; Subbi, J. *J. Phys. Chem.* **1991**, 95, 8482.
- (64) Geirer, A.; Wirtz, K. Z. *Naturforsch.* **1953**, A8, 532.
- (65) Dote, J. L.; Kivelson, D.; Schwartz, R. N. *J. Phys. Chem.* **1981**, 85, 2169.
- (66) Momicchioli, F.; Baraldi, B. *Chem. Phys.* **1988**, 123, 103.
- (67) It should be noted that fitting of the long-term rise to an exponential, i.e., a kinetic model, is not possible given the limited range of population times that yielded sufficiently high echo amplitudes to allow for an unambiguous construction of the 3PEPS curve.
- (68) Vanderzwan, G.; Hynes, J. T. *J. Phys. Chem.* **1985**, 89, 4181.
- (69) Horng, M. L.; Gardecki, J. A.; Papazyan, A.; Maroncelli, M. *J. Phys. Chem.* **1995**, 99, 17311.
- (70) Cho, B. M.; Carlsson, C. F.; Jimenez, R. *J. Chem. Phys.* **2006**, 124, 144905.